Simulating three-dimensional grapevine canopies and modelling their light interception characteristics

A.B. IANDOLINO[1], R.W. PEARCY[2] and L.E. WILLIAMS[1,3]

[1] Department of Viticulture and Enology, University of California, One Shields Avenue, Davis, CA 95616, USA
[2] Department of Evolution and Ecology, University of California, One Shields Avenue, Davis, CA 95616, USA
[3] University of California Kearney Agricultural Research and Extension Center, 9240 S. Riverbend Avenue, Parlier, CA 93648, USA
Corresponding author: Dr Larry Williams, email lewilliams@ucanr.edu

Abstract

Background and Aims: The objective of this study was to develop a simplified approach to simulate three-dimensional (3D) grapevine canopies and model light interception.

Methods and Results: A re-sampling procedure was developed to generate a set of allometric parameters based on their sample mean and distribution derived from shoots of field-grown vines grown in response to variable amounts of irrigation and N fertiliser. A large number of 3D models of grapevine canopies was reconstructed with the plant architecture model YPLANT based on re-sampled allometric parameters. Approximately 80% of intercepted light by the canopies was shown to be captured by 20–30% of the leaves, with deficit-irrigated and N-stressed plants having a greater proportion of leaf area exposed to high and moderate light intensity throughout the day compared with that of non-stressed vines. The amount of daily absorbed light increased with increasing leaf area per vine and was highly affected by row direction.

Conclusions: Model predictions agreed with previously reported and measured amounts and patterns of light interception.

Significance of the Study: The approach described here simplifies previous attempts to represent the 3D architecture of a grapevine canopy, provides a good approximation to conditions vines may experience in the field and may be of practical use for field research and/or optimisation of canopy management practices in commercial production systems.

Keywords: *canopy, light interception, modelling,* Vitis vinifera, *YPLANT*

Introduction

The dynamic and spatial pattern of light penetration, distribution and interception within a complex plant canopy depends on the physical interaction between incoming solar radiation and the three-dimensional (3D) distribution and optical properties of organs, such as leaves, fruits and stems (Ross 1981). The resulting heterogeneous light distribution has a profound effect not only on a plant's energy balance (Heilman et al. 1996), but also on multiple light-dependent developmental, physiological and metabolic processes at the single leaf and whole plant level (Chen et al. 2004, Shimazaki et al. 2007, Niinemets and Anten 2009). Predicting gradients of light interception and patterns within complex grapevine canopies is of great practical interest in viticulture. Changes in the amount of light intercepted and the environment within the canopy can affect its carbon balance (Smart 1973, 1974, Williams et al. 1994, Heilman et al. 1996, Mabrouk et al. 1997b) and water use (Katerji et al. 1994, Williams and Ayars 2005) as well as have a dramatic effect on biological processes defining productivity and fruit composition, such as bunch differentiation, berry size and concentration of sugars, flavonoids and aroma compounds (Williams and Matthews 1990, Mullins et al. 1992, Williams et al. 1994, Koch et al. 2012). Based on this practical knowledge, vineyard managers around the world frequently modify grapevine canopies via trellising, leaf removal, pruning and imposition of mild abiotic stresses (e.g. deficit irrigation and reduced N fertilisation) to optimise yield according to desired quality standards (Smart 1985, Smart and Robinson 1991).

Over the years, several methods have been developed to characterise the spatial distribution of organs within a grapevine canopy in order to understand better the effect of canopy management practices on the quantitative and qualitative productivity of different grape cultivars. Geometric models with a varying level of complexity have been used to estimate light interception by grapevine canopies (Smart 1973, Riou et al. 1989, Sinoquet et al. 1992). Those models assigned geometric shapes to canopy components and defined canopy properties based on shape attributes, such as size, spatial localisation, density and angle distributions. Subsequently, sunlight interception and attenuation were estimated with mathematical or statistical models. Alternative approaches to characterise better the spatial heterogeneity in the distribution of canopy organs are based on direct measurements, via 3D digitisation (Sinoquet et al. 1998, Falster and Westoby 2003, Pearcy et al. 2005) or by morphological and developmental rule-based simulations (Prusinkiewicz 1998, Birch et al. 2003, Allen et al. 2005). While these methods may increase accuracy and resolution, their

doi: 10.1111/ajgw.12036

application is often limited to small plants because of inadequate knowledge of developmental and allometric rules required for realistic reconstruction. As a result, canopy properties emerging from modelling plant-to-plant variability are often missed (Carbonneau and Cargnello 2003). To overcome these limitations, statistical models have been used to reconstruct 3D canopies based on parameter distributions inferred from sampled data (Casella and Sinoquet 2003, Potel et al. 2005, Louarn et al. 2008b). For example, Sonohat et al. (2006) reconstructed the 3D branching structure of a peach tree by combining the partial 3D digitising of the canopy and a rule-based model for the non-digitised areas based on known or assumed allometric relationships and the random sampling of shoot and/or organ attribute distribution. Louarn et al. (2008b) proposed a statistical reconstruction model that captures the spatial variability and heterogeneity of grapevine canopies based on probability distribution of measured attributes of different canopy components. Although these models provide a more realistic reconstruction of complex plant canopies, all require the implementation of complex algorithms using specialised programming language and software.

The objective of this study was to develop a simplified approach to simulate a 3D grapevine canopy and to apply the model to estimate the effects of deficit irrigation, N fertilisation and row orientation on canopy architecture and light interception. A re-sampling procedure was developed to generate a random set of simulated shoot and leaf allometric parameters. Sample mean and distribution were derived from randomly sampled shoots from field-grown vines grown under conditions that promote changes in canopy leaf area and density, such as deficit irrigation and variable N fertiliser rates. The plant architecture model YPLANT (Pearcy and Yang 1996, Pearcy et al. 2005, 2011) was used to reconstruct large numbers of 3D models of grapevine canopies based on re-sampled allometric parameters. The utility of YPLANT has recently been demonstrated in modelling light interception of woody plants as a function of plant diversity and structure (Lusk et al. 2011, 2012) and to ascertain determinants of light interception efficiency of small- to medium-sized plants (Duursma et al. 2012). The approach reported herein allowed us to capture plant-to-plant variability and generate a good approximation of light interception and attenuation patterns of field-grown vines as others have done with this model.

Materials and methods

Plant material, experimental conditions and design

The experiment was conducted during the 2001 and 2002 growing seasons in a commercial vineyard located 2 km north-west of Oakville (located in the Napa Valley), California, USA. The vineyard soil was a Bale clay loam with a 2–5% slope (Lambert and Kashiwagi 1978). Eight-year-old Cabernet Sauvignon (clone 8) grapevines (*Vitis vinifera* L.) grafted onto the rootstock 110R and trellised to a vertical shoot position (VSP) system were used in the study. Vine and row spacings were 1.0 and 1.83 m, respectively (5464 vines/ha). All cultural practices, with the exception of irrigation and N fertilisation, were applied by the vineyard manager. Vines were either irrigated on a weekly basis once midday leaf water potential reached a value of −1.0 MPa or not irrigated. The irrigated vines received applied water amounts at 100% of estimated crop evapotranspiration (ET_c) using the following equation:

$$ET_c = ET_o \times K_c \quad (1)$$

where ET_o equals reference evapotranspiration, and K_c is the crop coefficient (Allen et al. 1998). Reference ET data were obtained from the California Irrigation Management Information System weather station #77 (38° 26' N, 122° 25' W), located 2 km south of the experimental vineyard. The seasonal K_c values were a function of degree-days and had been developed for a VSP trellis on a 1.83-m row spacing with a maximum K_c value of 0.87 [see Williams (2010) for an example of the seasonal K_c used for a VSP trellis and a 3.05-m row spacing]. Water was applied via drip irrigation using two 2-L/h emitters per vine with the drip line attached to a wire positioned 0.3 m above the soil surface. Irrigation volume was calculated weekly, and the amount of water applied was measured with in-line water meters. The nitrogen (N) fertiliser treatments consisted of vines fertilised approximately 2 weeks prior to anthesis with potassium nitrate (KNO_3), 20 g N/vine (109 kg N/ha) and non-fertilised vines. The N fertiliser was placed below ground (0.15–0.20 m) under the emitters of each treatment vine and then covered with soil. Vines were irrigated for 4 h to facilitate distribution of the fertiliser into the root zone. The N fertiliser was applied to the same vines in both years of the study. The treatments were as follows: **00** – no applied water or N fertiliser; **0F** – no applied water, vines fertilised with N; **I0** – vines irrigated but no N fertiliser; and **IF** – vines irrigated and fertilised with N.

The same experimental design was replicated in two vineyards differing in row directions. The north-south experimental vineyard's rows (hereafter referred to as NS_E) had an azimuth of 310°, while the east-west experimental vineyard's rows (EW_E) had an azimuth of 225°. Three rows in each vineyard were selected for this experiment ($n = 3$). The treatment level randomisation was a two-step process: first a block of 18 vines within each row was randomly assigned to an irrigation level. Then, N fertiliser treatments were allocated to plots of nine vines within each irrigation treatment. The experimental unit consisted of the center seven vines in each irrigation × fertiliser plot and was used for data collection.

Development of a 3D vine architectural model and its implementation in YPLANT

Allometric shoot parameters required for the implementation of a 3D canopy architectural model in YPLANT (Pearcy and Yang 1996) were derived from randomly sampled shoots of field-grown vines in each vineyard/treatment combination, described above, in the second week of August 2002. The angle and azimuth of the leaf blade's surface normal and azimuth of the midrib for leaves at each node position were measured in the field from a set of five shoots in each experimental unit. The same five shoots were then brought to the laboratory, defoliated (for the determination of the area of individual leaves), and the value of internode length, diameter, elevation angle (α_s) and azimuth (ζ_s) in relation to true north was recorded for each node position along the primary (1°) shoot. Similar measurements were also taken at each node for petioles, with the exception of azimuth (ζ_p), which was considered for modelling purposes equivalent to that measured in the field for the subtending leaf. Lateral or secondary (2°) shoots were parameterised as described for 1° shoots except that leaf angles were assumed to have values similar to those of leaves on the 1° shoots. Leaf area per leaf for the 1° and 2° shoots was measured in sequential order from the base to the apex of the shoot using a LI-COR 1100 area meter (LI-COR Biosciences Inc., Lincoln, NE, USA).

A re-sampling procedure was devised to obtain random estimates of the parameters using the measured values. It was

assumed that linear and angular parameters used to construct the 3D architecture of the vine were normally distributed (Mabrouk et al. 1997b, Sonohat et al. 2006, Louarn et al. 2008b). The probability density function of the normal distribution was computed as follows:

$$f(x;\mu;\sigma) = p = \frac{1}{\sqrt{2\pi\sigma}} e^{-\left[\frac{(x-\mu)^2}{2\sigma^2}\right]} \quad (2)$$

where p represents the normal distribution of the probability density function values, x is a specific variable value, and μ and ς are the population mean and standard deviation, respectively. The equation used to solve for x was:

$$x = \mu + \sqrt{e^{\left[p\sqrt{2\pi\sigma}+\ln\left(2\sigma^2\right)\right]}} \quad (3)$$

Values of p were then obtained using the random number generator function RAND (range = 0–1) in MS Office Excel (Microsoft Inc., Seattle, WA, USA). Different values of x were obtained based on μ and ς assuming that these two population parameters were approximated by the sample mean and standard deviation, respectively. This re-sampling procedure generates sets of normally distributed linear and angular parameters describing leaf size and spatial location at each node position. An example of the implementation of the re-sampling procedure in MS Office Excel is as follows:

$$= \mathrm{ABS}(\mathrm{NORMSINV}(\mathrm{RAND}()) \times \mathrm{STDEV} + \mathrm{AVERAGE}) \quad (4)$$

where ABS, NORMSINV and RAND are MS Office Excel functions, and STDEV and AVERAGE refer to cells containing the mean and standard deviation of a given allometric parameter at a specific node along the shoot (see Figure S1).

The re-sampling procedure encoding the vine's canopy architecture was implemented as an MS Office Excel spreadsheet consisting of a set of four different submatrices: (i) parameter input; (ii) 1° shoot length; (iii) 2° shoot internode number; and (iv) the vine architecture file. The input submatrix was used to list linear (distance and length) and angular parameters (elevation and azimuth angles) of internodes, petioles and leaves at each node position. Input data consisted of the parameter means and standard deviations values at each node. The 1° shoot submatrix randomised node number per shoot and internode length, thus defining shoot length. The 2° shoot submatrix randomised the presence or absence of 2° shoots at each node along the 1° shoot as well as node number per 2° shoot. Finally, the vine architecture matrix re-sampled all parameter values simultaneously and generated a *.p (plant file) that was used by YPLANT to construct a 3D architectural model of a grapevine. Leaf shape features were defined by a set of Cartesian X-Y coordinates measured on representative 1° and 2° shoot leaves that were scanned and then digitised using SigmaScan Pro (Systat Software, Inc., Point Richmond, CA, USA). The basic vine architecture model consisted of a trunk, two 0.55-m cordons and three spurs per cordon. A 12-shoot vine resulted from two shoots at each spur position. Each shoot was modelled as an independent module. Secondary shoots were modelled as described for 1° shoots and then assigned to specific node positions as determined from shoots collected in the field.

Model implementation in YPLANT

YPLANT (Pearcy and Yang 1996) calculates the photon flux density (PFD) absorbed by the canopy by projecting light rays with the azimuth and elevation angles of the sun at specified intervals during the day. The trajectory of the sun was defined by the latitude of the location and day of the year. The Standard Overcast Sky (SOC) was used for the analysis of diffuse light absorbance by the canopy. The SOC algorithm simulates the diffuse light sky distribution as being brighter near the zenith than the horizon. The diffuse to global radiation ratio was set to 0.15. Light absorbed by the canopy was calculated from vectors originating from 160 different sky sectors (the combination of 8 different azimuth and 20 different zenith angles). The accuracy of the light interception subroutine has previously been validated (Pearcy and Yang 1996, Valladares and Pearcy 1998, Valladares and Pugnaire 1999). Leaf optical properties for light absorption calculation were based on data from Mabrouk et al. (1997b) for grapevines (leaf absorptance was set to 0.797 and reflectance to 0.122).

Simulations were conducted using 'vine models' parameterised from the different field treatments for the path of the sun on 1 August (day of the year 213) at a latitude of 38° 26' N (Oakville, CA, USA). This date was selected to exemplify model results because this day may be taken as an average for the onset of fruit ripening for Cabernet Sauvignon in the Napa Valley. Further vegetative growth at this stage of development is minimal because of vineyard management practices, such as hedging shoots growing above the top wire of the VSP trellis and/or deficit irrigation.

For each simulation, YPLANT generated an output file describing the amount of light absorbed by individual leaves in the canopy for each sample period throughout the day. Sample times were set every 10 min as this interval was found to be the optimum for maximum gain in accuracy while minimising computational time.

Canopy light attenuation gradients in field-grown and modelled vines

The light environment within the simulated canopies was modelled with a 'virtual quantum sensor grid' (see Figure S2) and then compared with the actual light attenuation patterns for field vines in the experimental vineyard. The virtual sensor grid was designed as a two-internode shoot emerging from a node located on the trunk of the vine. The first internode was horizontal and aligned to the row direction. The second internode was oriented vertically. At the apex of the second internode, 11 regularly spaced 'branches' emerged (every 0.05 m) horizontally and parallel to the canopy. 'Light sensors' in each branch were modelled as 30 1 cm^2 'diamond-shaped leaves' evenly distributed every 0.05 m along the branch. The absorbance of each 'leaf' on the branch was set equal to 100%. The 330 simulated leaves were used as PFD sensors taking advantage of YPLANT's ability to record light intercepted by individual leaves at specified sampling times during the sun's path. The PFD sensor grid could be moved up and down the canopy by modifying the height of the vertical branch. The above procedure allowed the characterisation of both diffuse light as well as direct beam penetration at different planes in the simulated canopies.

Direct measurement of light attenuation within the canopy was obtained on field-grown grapevines at the experimental site using a Sunfleck Ceptometer (Decagon, Pullman, WA, USA). The ceptometer was moved from the fruiting zone up the canopy in 0.2-m increments and each value recorded.

Simulation experiments conducted in YPLANT

Simulations were conducted for rows with an azimuth value of 310° (NS_E) and 225° (EW_E), the approximate row directions

at the experimental vineyard site. The leaf data set and vine architecture parameters of the **I0** treated vines were used to to simulate the effect of row orientation on light interception. Leaf angles were assumed to be independent of row orientation.

Experimental design and statistical analysis

The field experiment used a split-split-split plot factorial design (the first split was row direction; the second split was irrigation treatment and the third split was N fertiliser treatment) with complete randomised blocks distributed in three contiguous rows and two different row directions as described above. Statistical analyses were conducted using the statistical package in SAS Version 8 (SAS Institute Inc., Cary, NC, USA) for analysis of variance (PROC GLM) and Tukey's test for multiple comparisons of means. Hierarchical cluster analysis (HCA) and integration of the YPLANT results were conducted in Matlab Version 13R (The MathWorks Inc., Natick, MA, USA). The HCA (in Figure 9) was performed as described by Ewing et al. (1999). Briefly, a correlation matrix listing Pearson's correlation coefficient (r) between different leaves in the canopy was calculated for a particular variable (e.g. light absorbed at each sample time by the model). Then, a pairwise Euclidean distance matrix was recalculated based on r-values. Finally, leaves were clustered using Euclidean distances based on the unweighted pair group method with arithmetic mean algorithm (Sokal and Michener 1958). Non-linear regression equation fitting was conducted using SigmaPlot Version 8 (Systat Software, Inc.).

Results

Effects of irrigation and early season N fertiliser application on shoot and canopy architecture

Both irrigation and fertilisation strongly affected vine leaf area, with the irrigated (**I0**) and especially the irrigated and fertilised (**IF**) vines having a greater total vine leaf area than that of the non-irrigated, non-fertilised (**00**) vines (Table 1). This was due to a greater leaf area per leaf, particularly the upper leaves of the **IF** treatment's 1° shoots and greater leaf area development on 2° shoots in the **IF** and **I0** treatments (Figure 1). Growth of 2° shoots was restricted at the upper nodes of the **0F** and especially the **00** vines. Fertiliser application promoted growth of 2° shoots at the basal nodes of the 1° shoots. Leaves from the irrigated vines had a smaller leaf elevation angle (Table 1) and a random distribution of the leaf azimuth whereas leaves of the non-irrigated vines were preferentially oriented in a NE-SW axis (Figure 2).

Differences in shoot architecture because of the imposed treatments were used to generate 3D canopies simulating treatment effects on single shoots (Figure 3) and whole canopy architecture (Figure 4a,d). The procedure implemented to re-sample different allometric parameters measured on sampled shoots resulted in sets of ramdomly generated whole vine canopies (Figure 5).

Table 1. Allometric parameters for leaves and shoots of Cabernet Sauvignon grapevines grown in the NS_E rows in response to irrigation and N fertilisation treatments.

Parameter	Units/symbol	Treatment			
		00	**0F**	**I0**	**IF**
Leaves					
1° leaves/shoot	–	20.7 a	21.0 a	23.3 a	16.0 b
1° leaf area/shoot	cm^2	1952	2020	2192	2154
1° leaf area/leaf	cm^2	94.4 b	96.4 b	97.3 b	135.4 a
2° leaves/shoot	–	28.3 c	49.3 bc	74.7 ab	103 a
2° leaf area/shoot	cm^2	882 c	1974 bc	3431 ab	4464 a
2° leaf area/leaf	cm^2	31.1	39.5	46.9	43.3
Total leaf area/shoot	cm^2	2835 c	3967 bc	5623 ab	6619 a
Total leaf area/vine	m^2	3.4 c	4.8 bc	6.7 ab	7.9 a
1°/2° leaf area ratio	–	2.5 a	1.1 b	0.7 bc	0.5 c
Leaf elevation angle (east)	Degree ($E\alpha_l$)	79.1	81.5	65.3	66.2
Leaf elevation angle (west)	Degree ($W\alpha_l$)	75.1 a	77.4 a	50.2 c	60.1 b
Mean leaf elevation angle	Degree (α_l)	77.2 a	79.5 a	58.1 b	63.2 b
Leaf azimuth (east)	Degree ($E\zeta_l$)	107 b	170 a	100 b	117 ab
Leaf azimuth (west)	Degree ($E\zeta_l$)	268	305	284	273
Shoots					
Internode number	–	21.4	18.6	20.6	17.0
Internode length	cm	4.5	5.5	5.2	5.9
Shoot length	m	0.97	1.01	1.04	0.99
α_{shoot}	Degree	95.8	92.2	91.1	93.4

Means within an individual row followed by different letters are significantly different based on Tukey's test for multiple comparisons of means at $\alpha \leq 0.05$. Means within a row without letters are not significantly different. n = five shoots per vine except for total leaf area per vine where n = 12 shoots per vine. –, variable number; **00**, non-irrigated, non-fertilised; **0F**, non-irrigated, fertilised with N; 1°, primary; 2°, secondary; **I0**, irrigated, non-fertilised; **IF**, irrigated and fertilised with N; N, nitrogen.

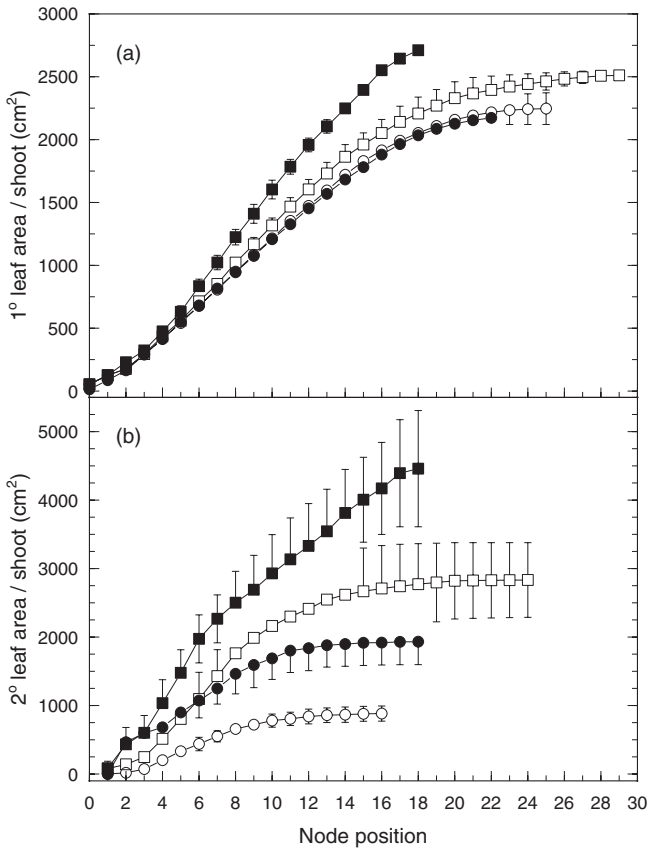

Figure 1. Effect of the treatment of vines with **00** – no irrigation and no N fertilisation (○), **0F** – no irrigation but fertilised with N (●), **I0** – irrigated but no N fertilisation (□) and **IF** – irrigated and fertilised with N (■) on (a) accumulated primary and (b) secondary leaf area measured along shoots of Cabernet Sauvignon from the basal to apical nodes at the onset of ripening or veraison. Each data point represents the mean of five shoots. Bars represent one standard error (SE) and are shown when larger than the symbol. The SE bars that overlap from one treatment to another are not shown.

The light environment within modelled and actual grapevine canopies

Measured and simulated values of the light environment within the grapevine canopies showed a defined pattern of light intensity attenuation from the top of the canopy downward into the fruiting zone (Figure 6). A large fraction of incoming solar radiation was attenuated in the uppermost (0.5–0.6 m) portion of the canopy in both cases. Light penetration into the fruiting zone was more severely attenuated for the modelled, N fertilised vines compared with that of the other treatments. The modelled, non-irrigated vines had greater light penetration into the upper portion of the canopy.

Modelled light interception as a function of water and N fertiliser applications

Maximum light interception for the NS_E row direction occurred mid-morning and mid- to late-afternoon (Figure 7). Instantaneous absorbed light per unit leaf area decreased with increasing leaf area per vine with the **IF** treatment having the lowest value (Figure 7a). Conversely, simulations predicted that as leaf area increased per vine greater total amounts of absorbed light per vine resulted (Figure 7b).

Irrigation and fertilisation substantially increased leaf area density (Table 2) and leaf area per shoot at the upper nodes. This high leaf area density resulted in greater self-shading and a more unequal distribution of light among leaves. Twenty-one per cent of the leaves for the modelled **IF** vines absorbed 80% of the daily light while for the **00**, **0F** and **I0** canopies 28% of the leaves absorbed the same proportion of light (Figure 8). An HCA illustrates the differing patterns of light absorption for leaves of vines in the **00** and **IF** treatments (Figure 9). Leaves of both modelled canopies can be grouped into discrete bunches based on the diurnal patterns of absorbed light. Most leaves of the modelled **00** treated vines received direct light at least once during the day. Most leaves of the IF-treatment vines, however, received only diffuse light.

Simulated light absorption efficiency decreased with increasing leaf area per vine (Figure 10) because of an increasing fraction of the total leaf area being self-shaded. While the general pattern held throughout the day, the differences were large enough to be significant only early in the morning or late in the afternoon for the NS_E row direction. The model predicted that approximately 2 h on either side of solar noon all treatments had a similar minimum light absorption efficiency. The minimum occurred because of the high fraction of self-shaded leaves at this time. In addition, the maximum value predicted for the morning was higher than that predicted by the model in the afternoon for all canopies. The maxima occur because of low solar angles as the leaves intercept more light than the reference horizontal surface. Simulated maximum light absorption efficiency early in the morning for the **00** treatment was almost double that of the **IF** treatment vines.

Effect of row direction on light interception

Modelled row direction effects showed that orientation influenced the amount of light intercepted by the canopy as well as the light absorption efficiency. Modelled vines in a true NS row intercepted more sunlight than vines in any other row direction at the latitude of the experimental vineyard (Figure 11a). Vines in a true EW row intercepted the least. The row directions of the two experimental vineyards used for field data collection absorbed similar amounts of light on a daily basis. The absorbed light value of these two row directions [310° (NS_E) and 225° (EW_E)] was 92 and 97%, respectively, of the maximum predicted by the model for a true NS row. The time at which the diurnal maxima of absorbed light occurred was also influenced by row direction (Figure 11a). The true NS row had a typical bimodal pattern with similar absorption maxima in the morning and afternoon while the true EW row had a single modal distribution. The bimodal maxima for the other two row directions differed between morning and afternoon. The morning was greater than the afternoon maximum for the 225° (EW_E) row direction while the opposite was true for the 310° (NS_E) row direction. The morning or afternoon maxima were greater when the sun azimuth was almost perpendicular to that particular row [see Figure 2 for the sun azimuth during the day in relation to the 310° (NS_E)] row direction. Modelled light absorption efficiency (ε) is predicted to be different among different treatments only during early morning or late afternoon when the sun was more perpendicular to the canopies, and ε is at its max for all treatments (Figure 11b). The true NS row had the greatest ε while the EW row direction the lowest. Two hours before and after solar noon, modelled ε was similar for all row orientations. At this time, ε also reached the diurnal minimum.

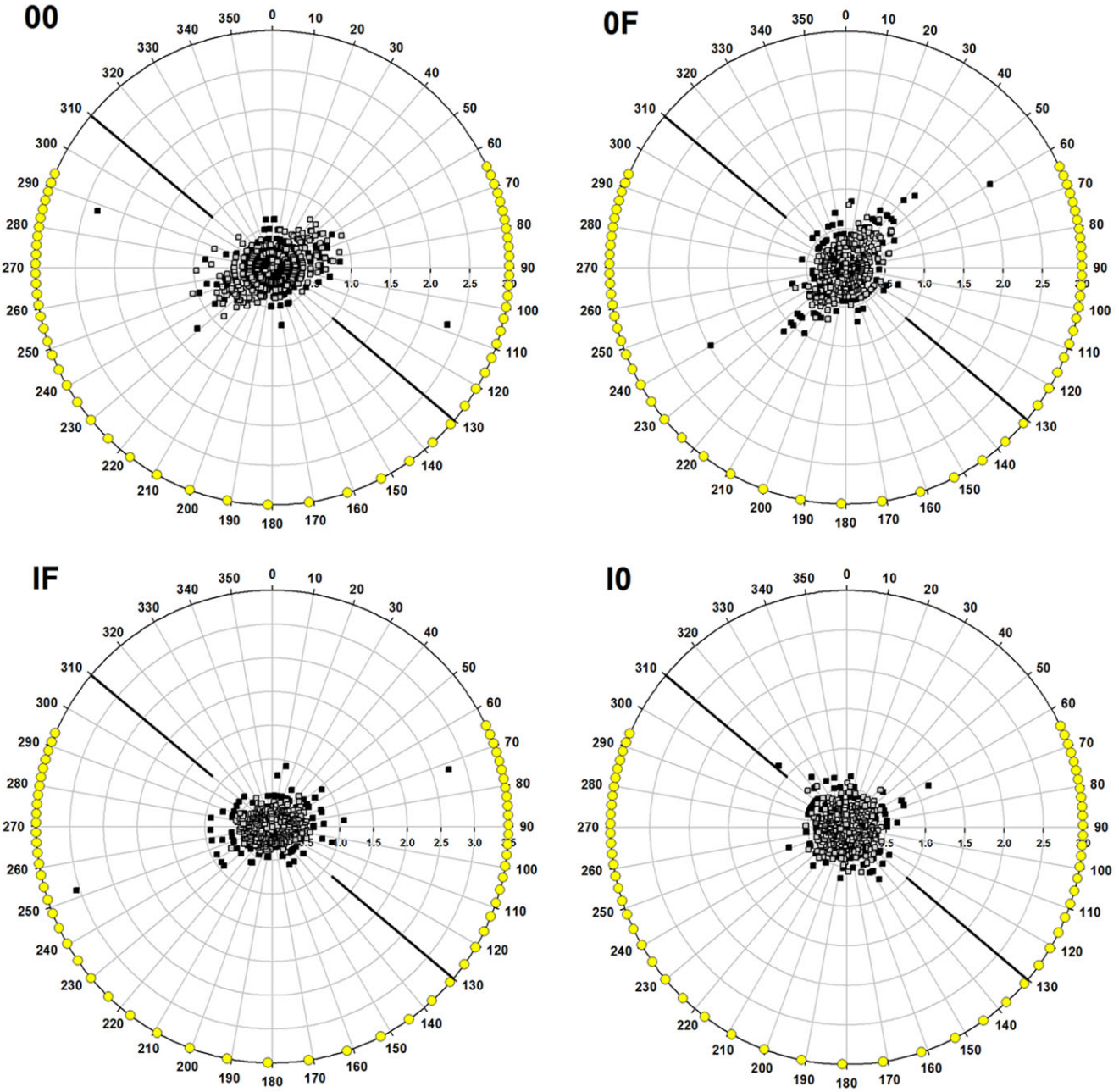

Figure 2. Leaf azimuth frequencies for 1° (▦) and 2° (■) leaves of the modelled vines treated with **00** – no irrigation and no N fertilisation, **0F** – no irrigation but fertilised with N, **I0** – irrigated but no N fertilisation and **IF** – irrigated and fertilised with N. Each data point represents the relative frequency (%) of leaves with a specific azimuth relative to the total number of leaves in the modelled canopy. Leaf azimuths in the modelled canopies result from the re-sampling procedure. In addition, each figure shows sun azimuths (●) in approximately 15-min intervals for 1 August (DOY 213) at Oakville (Latitude: 38°26'). The numerical values associated with the concentric circles represent percent values. The black line in each graph represents the row orientation (310°) of the experimental vineyard.

Discussion

The sensitivity of vegetative and reproductive organ growth rate and overall biomass accumulation to water (Schultz and Matthews 1988a,b, Winkel and Rambal 1993, Williams et al. 2010a,b) and N (Keller et al. 1998, 2001, Bell and Robson 1999) availability is well documented in grapevines and has practical management implication in commercial viticulture. In this study, variable water and N availability altered vegetative and reproductive growth modifying whole canopy architecture of field-grown grapevines (Iandolino 2004). For example, applied N fertiliser increased shoot internode length, leaf area and 2° shoot number while reduced water availability restricted 2° shoot growth and 2° leaf area development as it became a limiting growth factor later in the season. In addition, water and N availability increased 1° and 2° shoot leaf area because of their additive effect on increasing leaf size.

Estimated leaf area density for field and simulated vines ranged between 14 and 18 m^2/m^3. Leaf area density previously reported for grapevines range between 2 and 12 m^2/m^3 for non-divided and vertically divided canopies, respectively (Smart et al. 1985, Schultz 1995, Gladstone and Dokoozlian 2003).

The values for horizontally divided canopies range from 2 to 6 m^2/m^3 (Schultz 1995, Mabrouk et al. 1997a, Gladstone and Dokoozlian 2003, Louarn et al. 2008a). Localised leaf area density for confined grapevine canopies, however, can be as high as 8 (Schultz 1995), 15 (Sinoquet and Bonhomme 1992, Gladstone and Dokoozlian 2003) or 25 m^2/m^3 (Mabrouk et al. 1997a). Leaf area density of vines in this experiment, expressed per unit of canopy length, was at the upper end of the 2–12 m^2/m range reported for Cabernet Sauvignon vines from different sites in California (Dokoozlian and Kliewer 1995) but similar to those measured previously in this vineyard (Dr Larry Williams, pers. comm., 1999). This indicates a greater degree of canopy compactness in this study that would have affected canopy light interception per unit leaf area in both virtual and experimental vines.

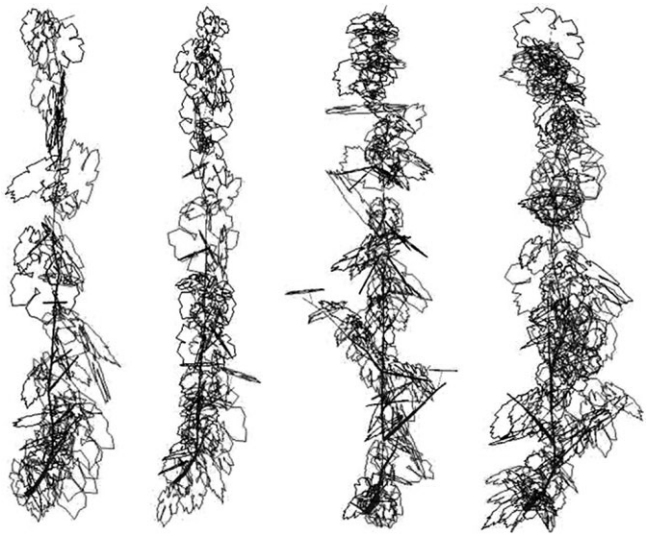

Figure 3. Modelled shoots of the vines treated with **00** – no irrigation and no N fertilisation, **0F** – no irrigation but fertilised with N, **I0** – irrigated but no N fertilisation and **IF** – irrigated and fertilised with N. Each shoot represents an example of shoots modelled based on allometric parameters measured from shoots in the field.

Leaf elevation (α_l) and azimuth (ζ_l) angles are among the most plastic traits of a plant's morphology (Lambers et al. 1998, Werner et al. 2001b, Falster and Westoby 2003) and are associated with optimisation of whole canopy light interception, carbon gain and avoidance of high temperature/irradiance-induced stress (Werner et al. 2001b). The adult shoot morphology of grapevines is characterised by a distichous phyllotaxy (Mullins et al. 1992). However, ζ_l can be modified in response to the local light environment because of leaf area density and gap frequency (Mabrouk et al. 1997a). Sampled leaves on the east side of the canopy in this study tended to be oriented to maximise light capture at a low sun elevation angle, while on the west side leaves tended to face the late afternoon sun (Figure 2). These trends are consistent with previously reported euphotometric (leaf blade oriented perpendicular to the sunbeam) behaviour of grapevine leaves (Smart 1974). The basal portion of shoots sampled from field-grown vines in this experiment had a greater frequency of leaves facing the inter-row space (data not shown). Leaf area density, however, was lower and leaves were oriented with an approximate 180° difference in the upper part of the shoot. Grapevine leaves have a characteristic plagiophile (mostly leaves with 45° α_l) distribution (Mabrouk et al. 1997b). Reported mean α_l values range between 53 and 58° in Merlot (Mabrouk et al. 1997b) and 45, 60–75 and 75° in Concord, Cabernet Sauvignon and Gewurztraminer, respectively (Smart 1985). The results from this study indicate that the mid-season α_l frequency of Cabernet Sauvignon was within reported values but it decreased for deficit-irrigated vines. Changes in α_l in response to water stress (Kao and Tsai 1998, Klein et al. 2001) and as a mechanism for avoidance of photoinhibition (Kao and Forseth 1991, 1992, Valladares and Pearcy 1997) have been reported for different plant species. Differences observed in α_l and ζ_l of plants are the result of diaheliotropic (solar tracking) and paraheliotropic (light avoiding) leaf movements to maximise carbon gain and minimise photoinhibition (Valladares and Pearcy 1997, Kao and Tsai 1998, Werner et al. 2001a). This data set represents α_l and ζ_l at

Table 2. Modelled allometric parameters describing shoot and canopy architecture in response to irrigation and N fertilisation treatments.

Parameter	Units	Treatment			
		00	0F	I0	IF
Leaf					
Area per vine	m^2	4.1 ± 0.9	5.3 ± 0.1	5.9 ± 0.3	8.7 ± 0.1
Leaf area density†	m^2/m^3	14.8 ± 0.1	14.2 ± 0.2	15.6 ± 0.2	18.0 ± 0.1
$1^o/2^o$ leaf area ratio	–	1.97 ± 0.2	0.99 ± 0.01	0.96 ± 0.01	0.59 ± 0.01
1^o leaf area per leaf	cm^2	99 ± 3.5	111 ± 1.2	112 ± 5.9	147 ± 1.2
2^o leaf area per leaf	cm^2	40 ± 3.1	42 ± 1.5	35 ± 0.7	46 ± 0.6
Leaf number/vine	–	618 ± 8	866 ± 7	1094 ± 17	1386 ± 17
α_l	Degree	73 ± 3	80 ± 1	61 ± 1	66 ± 1
Shoot					
Internode number	–	22.7 ± 0.2	19.7 ± 0.3	21.5 ± 0.4	18.2 ± 0.2
Internode length	cm	4.3 ± 0.2	5.4 ± 0.1	5.0 ± 0.3	5.9 ± 0.3
α_{shoot}	Degree	92 ± 4	94 ± 1	96 ± 1	96 ± 1

†Estimated from leaf area per shoot, shoots per vine and average canopy width. Values represent means ± standard error (n = 5). –, variable number; 00, non-irrigated, non-fertilised; 0F, non-irrigated, fertilised with N; 1°, primary; 2°, secondary; I0, irrigated, non-fertilised; IF, irrigated and fertilised with N.

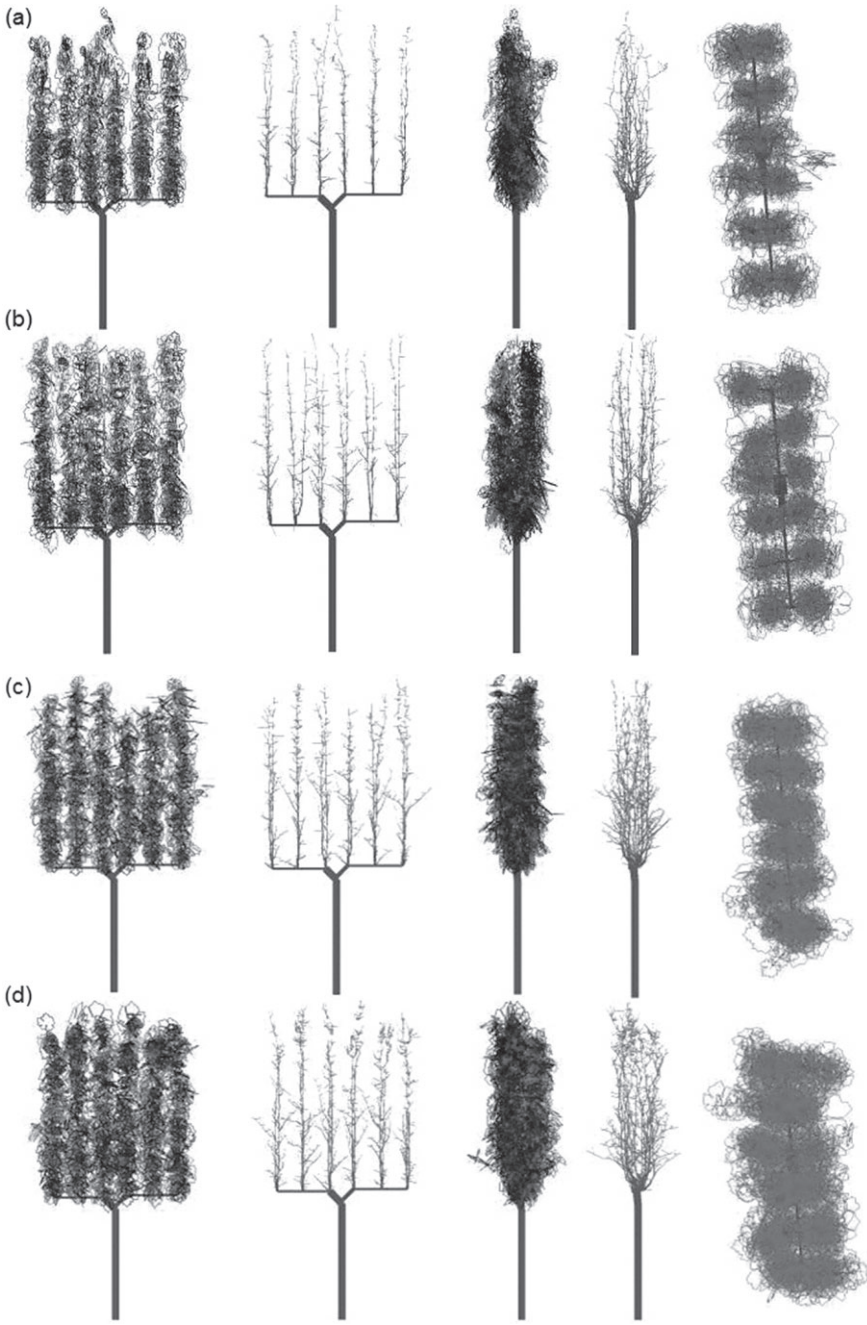

Figure 4. Representative modelled 3D canopies of the vines treated with (a) **00** – no irrigation and no N fertilisation, (b) **0F –** no irrigation but fertilised with N, (c) **I0** – irrigated but no N fertilisation and (d) **IF** – irrigated and fertilised with N. The same vine is shown with a lateral view and in the main row direction with and without leaves. In addition, an upper view of the canopies is also shown.

a specific time during vine development. Because ζ and α have a potentially significant impact on light absorption efficiency by single leaves and the whole canopy (Smart 1974, Pearcy and Yang 1996), there is a clear need for a better understanding of grapevine leaf angle tropisms in response to abiotic stresses and the local and diurnal variability of the light environment.

Individual shoots and canopies of grapevines positioned by a VSP trellis simulated in this study were similar to those seen in the field (personal observations) and in the literature (Mullins et al. 1992, Louarn et al. 2008b). Simulations of these grapevine canopies by YPLANT were accomplished by converting a finite number of allometric parameters into a virtually infinite number of possible parameter combinations. Because the required individual angular and linear values are calculated from the mean and standard deviation of measurements on the experimental vines, the modelled parameter value distributions are best estimates of the actual allometric parameters that define the architecture of a canopy. This approach significantly reduces the complexity of the direct sampling of allometric parameters on large plant canopies, and as such avoids the requirement of complex algorithms and specialised software to reconstruct different vine canopies (Louarn et al. 2008a,b).

Light attenuation and shade within grapevine canopies can be modified by manipulating vegetative growth, shoot number, leaf area density and the 3D arrangement of the canopy using different trellising systems (Smart 1974, Louarn et al. 2008a). Indices presently used in viticulture to characterise the spatial heterogeneity of leaf area density (Smart 1985, Mabrouk et al. 1997a) do not reflect the complex nature of grapevine canopies in terms of leaf elevation and azimuth angles, leaf age, shade/sun leaf type and the extent of leaf overlapping (Riou et al. 1989, Schultz 1995, Mabrouk et al. 1997a, Zufferey et al. 2000).

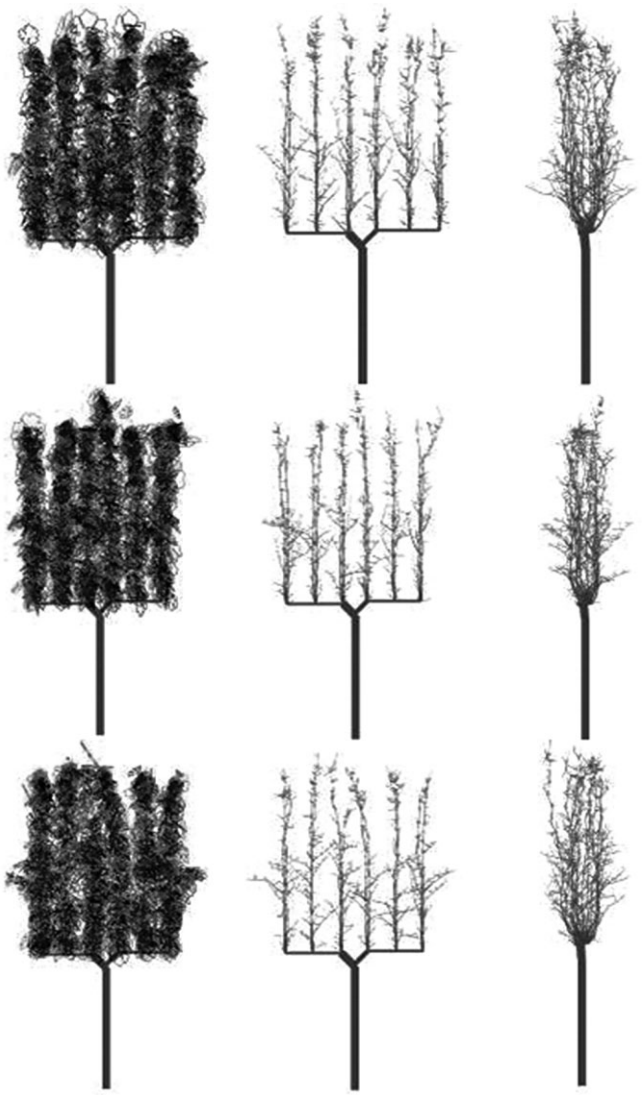

Figure 5. Model output of the variation in canopies based on the basic architecture of vines treated with **IF** – irrigated and fertilised with N. Vines are shown from the lateral side with and without leaves and in the main row direction. Changes in leaf and shoot angles take place as a result of the re-sampling routine.

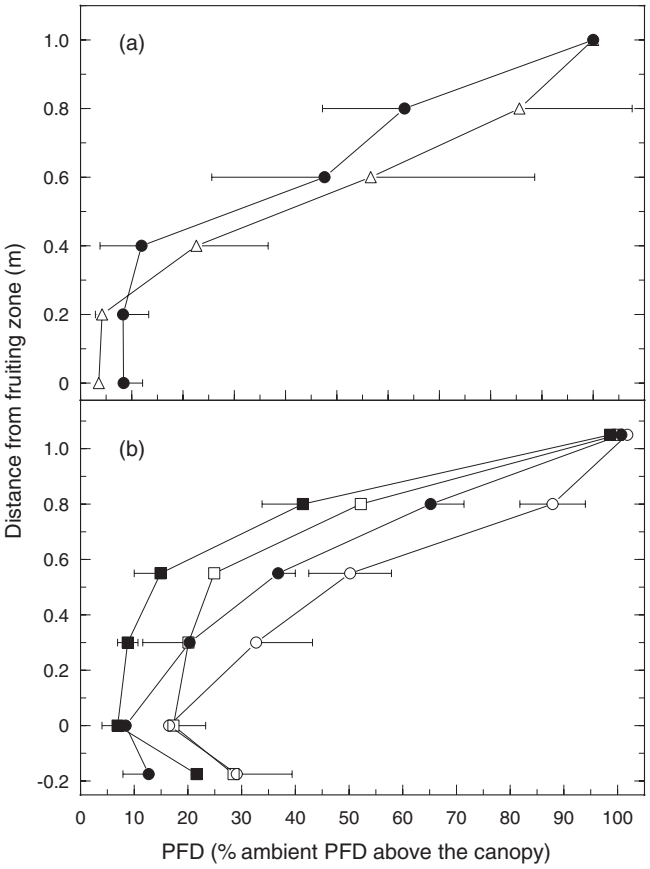

Figure 6. (a) Average light attenuation profile measured between berry set and veraison for field-grown Cabernet Sauvignon vines with EW_E and NS_E row direction and (b) that modelled at veraison with a virtual photon flux density sensor grid and the following treatments **00** – no irrigation and no N fertilisation (○), **0F** – no irrigation but fertilised with N (●), **I0** – irrigated but no N fertilisation (□) and **IF** – irrigated and fertilised with N (■). Data sampled from field-grown vines represent values collected at solar noon with a ceptometer placed at different heights within the canopy parallel to the cordon direction. Modelled data represent mean values sampled between 900 and 1500 Pacific Daylight Time for 1 August at Oakville (Latitude: 38°43'). Each point in the modelled results represents the mean value of the five central PFD sensor lines (0.15 m at each side of the cordon).

The model output for light absorbed by single leaves demonstrated that leaves within the canopy may experience different light absorption patterns throughout the day. Modelled light attenuation profiles within the canopy reported here are in agreement with field measurements taken in this study and those reported by others (Dokoozlian and Kliewer 1995, Mabrouk et al. 1997b, Gladstone and Dokoozlian 2003, Louarn et al. 2008a). Modelled light intensity within the bunch zone ranged between 7 and 20% of incoming PFD measured at the top of the canopy with the range dependent upon canopy leaf area density. The amount of light absorbed daily by individual leaves impact photosynthetic responses (Farquhar and von Caemmerer 1982, Sims and Pearcy 1993, Schultz 2003, Niinemets et al. 2004), which are important when scaling up from single leaves to the whole canopy (De Pury and Farquhar 1997, Thornley 2002).

Leaf acclimation to the sun and shade is even more important in modelling whole-vine net CO_2 assimilation (A_n) because the amount of leaf area in constant shade within a confined grapevine canopy may be as high as 50% of the total leaf area (Schultz 1995, Escalona et al. 2003, Louarn et al. 2008b). A large proportion of the intercepted light (~80%) was captured by a relatively small number of leaves (20–30%) for the modelled grapevine canopies in this study. The estimates generated from the model used here are in agreement with reported values for dense grapevine canopies where only 19% of the total leaf area was estimated to intercept direct light and approximately 70% of the direct light absorption was by the outer leaf layers (Smart 1974).

Early morning and late afternoon light absorption efficiencies (ε) ranged between 0.34 and 0.78 depending on row direction and leaf area density in this study. Geometric canopy models predict ε values ranging from 0.3 to 0.85 at those times (Riou et al. 1989, Mabrouk et al. 1997b). Around solar noon, modelled values of 0.06–0.08 were independent of row direction or changes in leaf area density. Geometric models predict

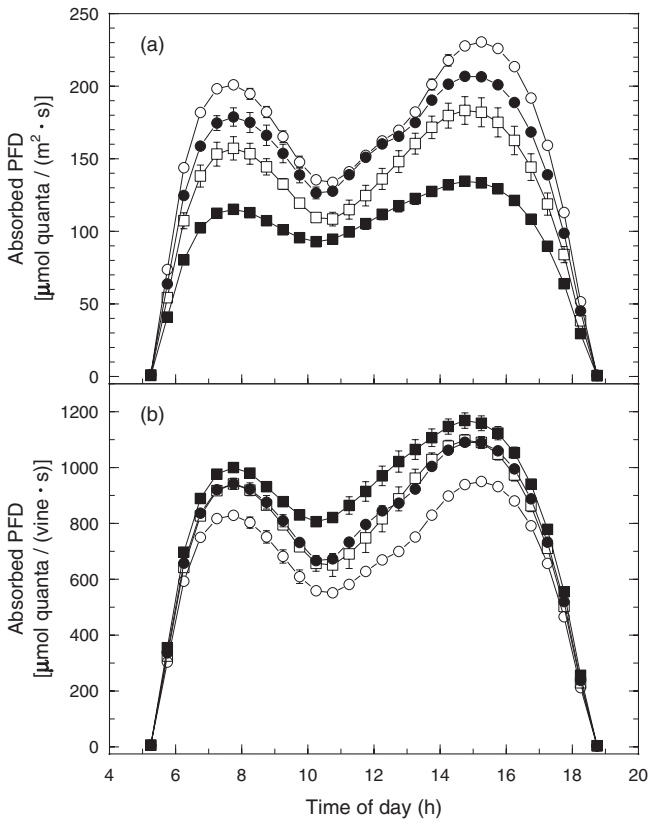

Figure 7. Modelled diurnal (Pacific Daylight Time) trends in estimated canopy photon flux density absorption for treatments **00** – no irrigation and no N fertilisation (○), **0F** – no irrigation but fertilised with N (●), **I0** – irrigated but no N fertilisation (□) and **IF** – irrigated and fertilised with N (■) in the NS_E oriented rows. Values were generated every 30 min and are expressed on (a) a leaf area or (b) a vine basis. Each value represents the mean output of three different modelled vines per treatment. Results are model predictions for 1 August at Oakville. Modelled daily absorbed light values are 32.7 (○), 38.2 (●), 37.8 (□) and 41.9 (■) mol/vine for data presented in (b).

greater ε values at solar noon ranging from 0.25 to 0.50 (Riou et al. 1989, Mabrouk et al. 1997b). The differences reported here and those of the geometric models may arise from variations in displayed area at solar noon among the different modelled canopy configurations used. The 3D representation of canopies in YPLANT can potentially provide a better representation of canopy gaps and heterogeneity in leaf area distribution than those in geometrical models (Riou et al. 1989, Sinoquet et al. 1992).

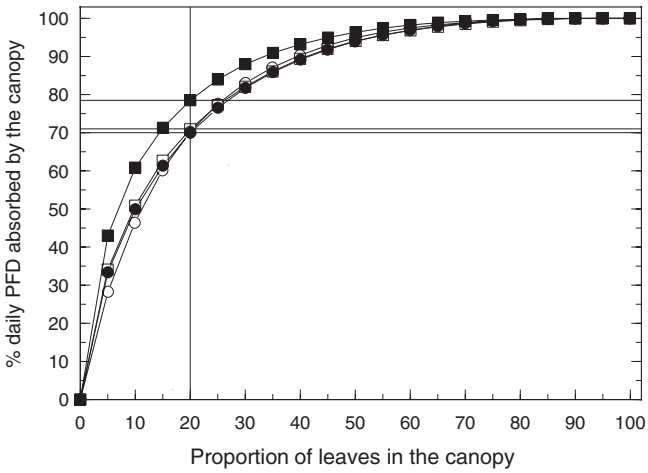

Figure 8. Effect of the treatments **00** – no irrigation and no N fertilisation (○), **0F** – no irrigation but fertilised with N (●), **I0** – irrigated but no N fertilisation (□) and **IF** – irrigated and fertilised with N (■) on the proportion of daily, absorbed light by leaves in the modelled canopies for NS_E oriented rows. Values represent the mean of three different modelled canopies per treatment. The horizontal lines represent the proportion daily photon flux density absorbed by 20% of the leaves in the canopy of the four treatments. Two of the treatments (**00** and **0F**) had the same value.

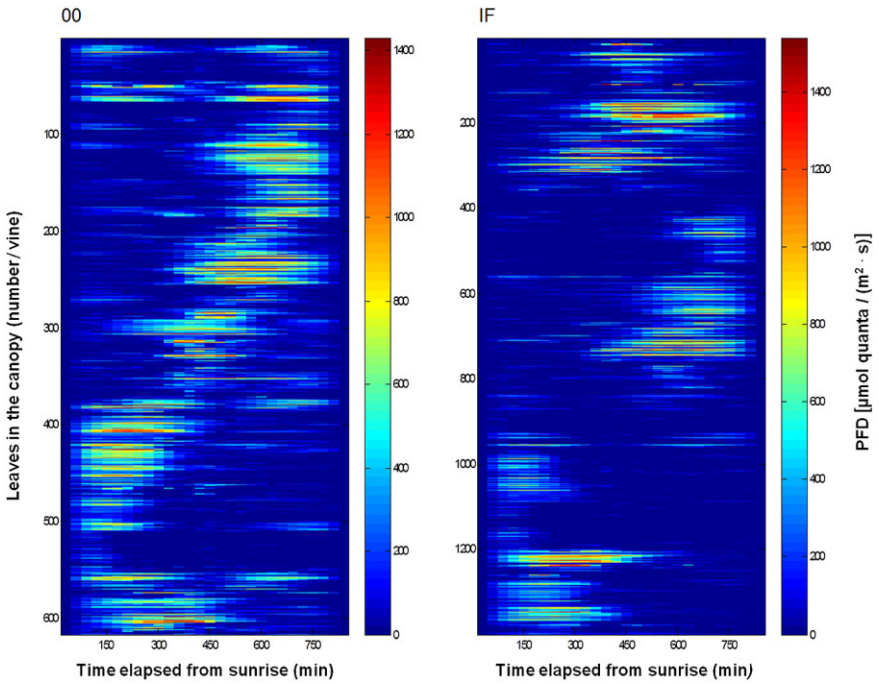

Figure 9. Hierarchical cluster analysis describing the effect of **00** – no irrigation or N fertilisation and **IF** – irrigated and fertilised with N treatments on the patterns of light absorption by different leaves in the two modelled canopies throughout the sun path of 1 August at Oakville, CA. Colour scale indicates the amount of absorbed light at each sampling point per leaf (set in YPLANT every 30 min from sunrise to sunset, 28 total or two samples/h). Note that the modelled canopies have different numbers of leaves on the *Y*-axis (616 and 1419 for the **00** and **IF** treatments, respectively).

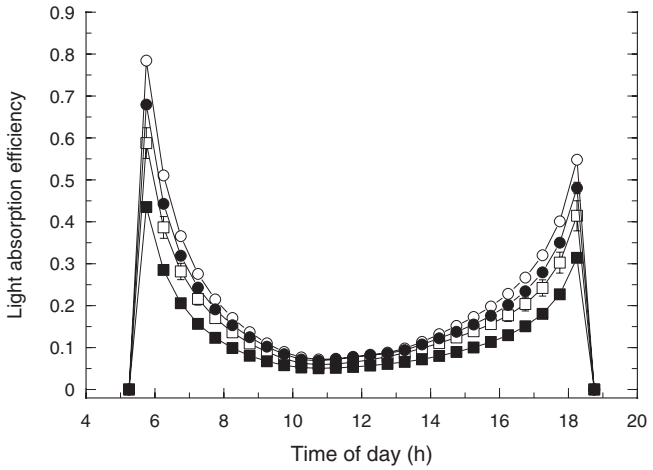

Figure 10. Effect of the treatments **00** – no irrigation and no N fertilisation (○), **0F** – no irrigation but fertilised with N (●), **I0** – irrigated but no N fertilisation (□) and **IF** – irrigated and fertilised with N (■)on the diurnal trends in light absorption efficiency [relative ratio between the mean absorbed photon flux density (PFD) by the canopy in relation to the PFD incident on a horizontal plane (Pearcy and Yang 1996)] for NS oriented rows. Each value represents the mean output of three different modelled vines per treatment. Results are model predictions for 1 August at Oakville, CA.

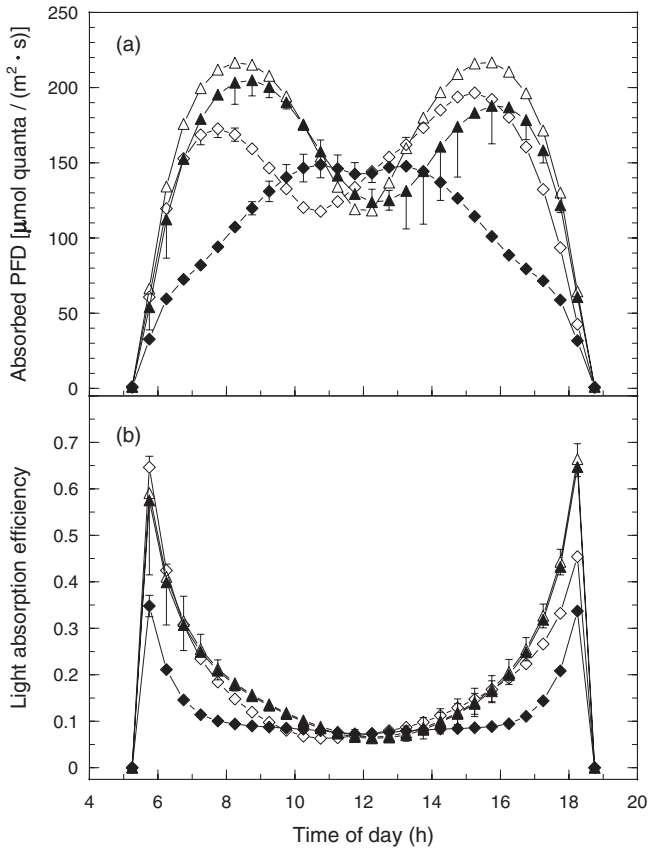

Figure 11. Effect of row orientation [(Δ) 0–180°, (▲) 45–225°, (◆) 90–270° and (◊) 130–310°] on diurnal trends of (a) modelled absorbed light and (b) light absorption efficiency. Modelled daily absorbed light values are (Δ) 41.6, (▲) 40.4, (◆) 28.3 and (◊) 38.1 mol/vine for data presented in (a). The **I0** treatment was the canopy used to run the simulations across row orientation.

Summary

A simplified modelling approach to reconstruct complex 3D plant canopies was developed by implementing a statistical re-sampling procedure in a spreadsheet application (MS Excel) and YPLANT (Pearcy and Yang 1996). The modelling approach generates an infinite number of grapevine canopies based on a fixed set of allometric parameters whose frequency distribution properties are estimated from sampled shoots or known allometric rules. The model was parameterised using data collected from vines receiving variable amounts of water and N fertiliser and grown in two contrasting row orientations. The model provided a good approximation to measured or previously reported values of light variability, attenuation gradients and overall light interception by complex grapevine canopies.

This modelling approach has several advantages over purely geometric models. First, it increases the 3D canopy modelling scale range from single-leaf to whole-canopy level. In addition, the statistical re-sampling method introduces a better representation of within vine and vine-to-vine variabililty in allometric parameters. As a result, this model allows a single-leaf level to whole-canopy resolution of the interaction with intercepted sunflecks enabling the evaluation of practical viticultural questions such as the effect of leaf removal or trellis system on the light environment within the fruiting zone. The model has also advantages over more complex statistical reconstruction models based on more elaborate algorithms and specialised software. The implementation of the re-sampling procedure on a widely available software platform (MS Excel) simplifies model re-parameterisation making the model accessible to a wider range of viticulture researchers. Moreover, the YPLANT permits single-leaf parametisation of a biochemical model of photosynthesis (Farquhar et al. 1980). The increased 3D modelling resolution coupled with the possibility of modelling single-leaf photosynthetic rate based on light interception opens the possibility to estimate whole-vine C assimilation.

Acknowledgements

This research was supported in part by grants from the American Vineyard Foundation, Viticulture Consortium and the California Competitive Grants for Viticulture and Enology. We thank the Robert Mondavi Winery and in particular Daniel Bosch and all the vineyard management technical staff for their support.

References

Allen, M.T., Prusinkiewicz, P. and DeJong, T.M. (2005) Using L-systems for modeling source-sink interactions, architecture and physiology of growing trees: the L-PEACH model. New Phytologist **166**, 869–880.

Allen, R.A., Pereira, L.S., Raes, D. and Smith, M. (1998) Crop evapotranspiration: guidelines for computing crop water requirements. FAO irrigation and drainage paper 56 (Food and Agriculture Organization: Rome, Italy).

Bell, S.J. and Robson, A. (1999) Effect of nitrogen fertilization on growth, canopy density, and yield of *Vitis vinifera* L. cv. Cabernet Sauvignon. American Journal of Enology and Viticulture **50**, 351–358.

Birch, C.J., Andrieu, B., Fournier, C., Vos, J. and Room, P. (2003) Modelling kinetics of plant canopy architecture – concepts and applications. European Journal of Agronomy **19**, 519–533.

Carbonneau, A. and Cargnello, G. (2003) Architecture de la vigne et systémes de conduit (Dunod Ed.: Paris, France).

Casella, E. and Sinoquet, H. (2003) A method for describing the canopy architecture of coppice poplar with allometric relationships. Tree Physiology **23**, 121–133.

Chen, M., Chory, J. and Fankhauser, C. (2004) Light signal transduction in higher plants. Annual Review of Genetics **38**, 87–117.

De Pury, D.G.G. and Farquhar, G.D. (1997) Simple scaling of photosynthesis from leaves to canopies without the errors of big-leaf models. Plant, Cell and Environment **20**, 537–557.

Dokoozlian, N.K. and Kliewer, W.M. (1995) The light environment within grapevine canopies. II. Influence of leaf area density on fruit zone light environment and some canopy assessment parameters. American Journal of Enology and Viticulture **46**, 219–226.

Duursma, R.A., Falster, D.S., Valladares, F., Sterck, F.J., Pearcy, R.W., Lusk, C.H., Sendall, K.M., Nordenstahl, M., Houter, N.C., Atwell, B.J., Kelly, N., Kelly, J.W.G., Liberloo, M., Tissue, D.T., Medlyn, B.E. and Ellsworth, D.S. (2012) Light interception efficiency explained by two simple variables: a test using a diversity of small- to medium-sized woody plants. New Phytologist **193**, 397–408.

Escalona, J.M., Flexas, J., Bota, J. and Medrano, H. (2003) Distribution of leaf photosynthesis and transpiration within grapevine canopies under different drought conditions. Vitis **42**, 57–64.

Ewing, R.M., Kahla, A.B., Poirot, O., Lopez, F., Audic, S. and Claverie, J.M. (1999) Large-scale statistical analyses of rice ESTs reveal correlated patterns of gene expression. Genome Research **9**, 950–959.

Falster, D.S. and Westoby, M. (2003) Leaf size and angle vary widely across species; what consequences for light interception? New Phytologist **158**, 509–525.

Farquhar, G.D. and von Caemmerer, S. (1982) Modelling of photosynthetic response to environmental conditions. In: Encyclopedia of plant ecology II. Water relations and carbon assimilation 12B. Eds. O.L. Lange, P.S. Nobel, C.B. Osmond and H. Ziegler (Springer-Verlag: Berlin, Germany) pp. 540–587.

Farquhar, G.D., von Caemmerer, S. and Berry, J.A. (1980) A biochemical model of photosynthetic CO_2 assimilation in leaves of C_3 species. Planta **149**, 78–90.

Gladstone, E.A. and Dokoozlian, N.K. (2003) Influence of leaf area density and trellis/training system on the light microclimate within grapevine canopies. Vitis **42**, 123–131.

Heilman, J.L., McInnes, K.J., Gesch, R.W., Lascano, R.J. and Savage, M.J. (1996) Effects of trellising on the energy balance of a vineyard. Agricultural and Forest Meteorology **81**, 79–83.

Iandolino, A.B. (2004) Abiotic stress effects on the grapevine (*Vitis vinifera* L.) canopy's carbon balance and metabolic profile of flavonoids in berries. PhD Thesis, University of California, Davis, CA, USA. 453 pp.

Kao, W.Y. and Forseth, I.N. (1991) The effects of nitrogen, light and water availability on tropic leaf movements in soybean (*Glycine max*). Plant, Cell and Environment **14**, 287–293.

Kao, W.Y. and Forseth, I.N. (1992) Diurnal leaf movement, chlorophyll fluorescence and carbon assimilation in soybean grown under different nitrogen and water availability. Plant, Cell and Environment **15**, 703–710.

Kao, W.Y. and Tsai, T.T. (1998) Tropic leaf movements, photosynthetic gas exchange, leaf $\delta^{13}C$ and chlorophyll a fluorescence of three soybean species in response to water availability. Plant, Cell and Environment **21**, 1055–1062.

Katerji, N., Daudet, F.A., Carbonneau, A. and Ollat, N. (1994) Etudè à l'échelle de la plante entière du fonctionnement hydrique et phosynthétique de la vigne: comparison des systemes de conduite traditionnel et en lyre. Vitis **33**, 197–203.

Keller, M., Arnink, K.J. and Hrazdina, G. (1998) Interaction of nitrogen availability during bloom and light intensity during veraison. I. Effects on grapevine growth, fruit development, and ripening. American Journal of Enology and Viticulture **49**, 333–340.

Keller, M., Kummer, M. and Vasconcelos, M.C. (2001) Reproductive growth of grapevines in response to nitrogen supply and rootstock. Australian Jounal of Grape and Wine Research **7**, 12–18.

Klein, I., Esparza, G., Weinbaum, S. and DeJong, T.M. (2001) Effects of irrigation deprivation during the harvest period on leaf persistence and function in mature almond trees. Tree Physiology **21**, 1063–1072.

Koch, A., Ebeler, S., Williams, L. and Matthews, M. (2012) Fruit ripening in *Vitis vinifera*: light intensity before and not during ripening determines the concentration of 2-methoxy-3-isobutylpyrazine in Cabernet Sauvignon berries. Physiologia Plantarum **145**, 275–285.

Lambers, H., Chapin, III F.S. and Pons, T.L. (1998) Plant physiological ecology (Springer-Verlag: New York, NY, USA).

Lambert, D.W. and Kashiwagi, J.H. (1978) Soil survey of Napa County, California (United States Department of Agriculture – Natural Resources Conservation Service: Washington, DC, USA).

Louarn, G., Dauzat, J., Lecoeur, J. and Lebon, E. (2008a) Influence of trellis system and shoot positioning on light interception and distribution in two grapevine cultivars with different architectures: an original approach based on 3D canopy modelling. Australian Journal of Grape and Wine Research **14**, 143–152.

Louarn, G., Lecoeur, J. and Lebon, E. (2008b) A three dimensional statistical reconstruction model of grapevine (*Vitis vinifera*) simulating canopy structure variability within amd between cultivar/training system pairs. Annals of Botany **101**, 1167–1184.

Lusk, C.H., Sendall, K. and Kooyman, R. (2011) Latitude, solar elevation angles and gap-regenerating rain forest pioneers. Journal of Ecology **99**, 491–502.

Lusk, C.H., Pérez-Millaqueo, M.M., Saldaña, A., Bruns, B.R., Laughlin, D.C. and Falster, D.S. (2012) Seedlings of temperate rainforest conifer and angiosperm trees differ in leaf area display. Annals of Botany **110**, 177–188.

Mabrouk, H., Carbonneau, A. and Sinoquet, H. (1997a) Canopy structure and radiation regime in grapevine. I. Spatial and angular distribution of leaf area in two canopy systems. Vitis **36**, 119–123.

Mabrouk, H., Carbonneau, A. and Sinoquet, H. (1997b) Canopy structure and radiation regime in grapevine. II. Modeling radiation interception and distribution within the canopy. Vitis **36**, 125–132.

Mullins, M.G., Bouquet, A. and Williams, L.E. (1992) Biology of the grapevine (University Press: Cambridge, England).

Niinemets, U. and Anten, N.P.R. (2009) Packing the photosynthetic machinery: from leaf to canopy. Laisk, A., Nedbal, L. and Govindjee, eds. Photosynthesis in silico: understanding complexity from molecules to ecosystems. Volume 29. Advances in photosynthesis and respiration. (Springer: Dordrecht, The Netherlands) pp. 363–399.

Niinemets, U., Kull, O. and Tenhunen, J.D. (2004) Within-canopy variation in the rate of development of photosynthetic capacity is proportional to integrated quantum flux density in temperate deciduous trees. Plant, Cell and Environment **27**, 293–313.

Pearcy, R.W. and Yang, W. (1996) A three-dimensional crown architecture model for assessment of light capture and carbon gain by understorey plants. Oecologia **108**, 1–12.

Pearcy, R.W., Muraoka, H. and Valladares, R. (2005) Crown architecture in sun and shade envrionments: assessing function and trade-offs with a three-dimensional simulation model. New Phytologist **166**, 791–800.

Pearcy, R.W., Duursma, R.A., Falster, D.S. and PrometheusWiki contributors (2011) Studying plant architecture with YPLANT and 3D digitising. PrometheusWiki. http://prometheuswiki.publish.csiro.au/tikiindex.php?page=Studying+plant+architecture+with+Yplant+and+3D+digitising [accessed 18/07/13].

Potel, C., Monney, P., Sinoquet, H., Sonohat, G. and Lauri, P.E. (2005) Digitalisation tridimensionnelle des arbres pour l'analyse de systèmes de vergers de pommier. Revue Suisse de Viticulture d'Aboriculture et d'Horticulture **37**, 173–179.

Prusinkiewicz, P. (1998) Modeling of spatial structure and development of plants: a review. Scientia Horticulturae **74**, 113–149.

Riou, C., Valancogne, C. and Pieri, P. (1989) Un modele simple d'interception du rayonnement solaire par la vigne – verification experimentale. Agronomie **9**, 441–450.

Ross, J. (1981) The radiation regime and architecture of plant stands (Dr. W. Junk Publishers: The Hague, The Netherlands).

Schultz, H.R. (1995) Grape canopy structure, light microclimate and photosynthesis. I. A two dimensional model of the spatial distribution of surface area densities and leaf ages in two canopy systems. Vitis **34**, 211–215.

Schultz, H.R. (2003) Extension of a Farquhar model for limitations of leaf photosynthesis induced by light environment, phenology and leaf age in grapevines (*Vitis vinifera* L. cvs. White Riesling and Zinfandel). Functional Plant Biology **30**, 673–687.

Schultz, H.R. and Matthews, M.A. (1988a) Vegetative growth distribution during water deficits in *Vitis vinifera* L. Australian Journal of Plant Physiology **15**, 641–656.

Schultz, H.R. and Matthews, M.A. (1988b) Resistance to water transport in shoots of *Vitis vinifera* L. Relation to growth at lower water potential. Plant Physiology **88**, 718–724.

Shimazaki, K., Doi, M., Assmann, S.M. and Kinoshita, T. (2007) Light regulation of stomatal movement. Annual Review of Plant Biology **58**, 219–247.

Sims, D.A. and Pearcy, R.W. (1993) Sunfleck frequency and duration affects growth rate of the understorey plant, *Alocasia macrorrhiza*. Functional Ecology **7**, 683–689.

Sinoquet, H. and Bonhomme, R. (1992) Modelling radiative transfer in mixed and row inter-cropping systems. Agricultural and Forest Meteorology **62**, 219–240.

Sinoquet, H., Valancogne, C., Lescure, A. and Bonhomme, R. (1992) Modelisation de l'interception des rayonnements solaires dans culture en rangs. III. Application a une vigne traditionnelle. Agronomie **12**, 307–318.

Sinoquet, H., Thanisawanyangkura, S., Mabrouk, H. and Kasemsap, P. (1998) Characterization of the light environment in canopies using 3D digitizing and image processing. Annals of Botany **82**, 203–212.

Smart, R.E. (1973) Sunlight interception by canopies. American Journal of Viticulture and Enology **24**, 141–147.

Smart, R.E. (1974) Photosynthesis by grapevine canopies. Journal of Applied Ecology **11**, 997–1006.
Smart, R.E. (1985) Principles of grapevine canopy microclimate manipulation with implications for yield and quality. A review. American Journal of Enology and Viticulture **36**, 230–239.
Smart, R.E. and Robinson, M.D. (1991) Sunlight into the wine (Winetitles: Adelaide, SA, Australia).
Smart, R.E., Robinson, J.B., Due, G.R. and Brien, C.J. (1985) Canopy microclimate modification for the cultivar Shiraz.I. Definition of canopy microclimate. Vitis **24**, 17–31.
Sokal, R. and Michener, C. (1958) A statistical method for evaluating systematic relationships. University of Kansas Scientific Bulletin **28**, 1409–1438.
Sonohat, G., Sinoquet, H., Kulandaivelu, V., Combes, D. and Lescourret, F. (2006) Three-dimensional reconstruction of partially 3D-digitized peach tree canopies. Tree Physiology **26**, 337–351.
Thornley, J.H.M. (2002) Instantaneous canopy photosynthesis: analytical expressions for sun and shade leaves based on exponential light decay down the canopy and an acclimated non-rectangular hyperbola for leaf photosynthesis. Annals of Botany **89**, 451–458.
Valladares, F. and Pearcy, R.W. (1997) Interactions between water stress, sun-shade acclimation, heat tolerance and photoinhibition in the sclerophyll *Heteromeles arbutifolia*. Plant, Cell and Environment **20**, 25–36.
Valladares, F. and Pearcy, R.W. (1998) The functional ecology of shoot architecture in sun and shade plants of *Heteromeles arbutifolia* M. Roem., a Californian chaparral shrub. Oecologia **114**, 1–10.
Valladares, F. and Pugnaire, F.I. (1999) Trade-offs between irradiance capture and avoidance in semi-arid environments assessed with a crown architecture model. Annals of Botany **83**, 459–469.
Werner, C., Ryel, R.J. and Beyschlag, W. (2001a) Effects of photoinhibition on whole-plant carbon gain assessed with a photosynthesis model. Plant, Cell and Environment **24**, 27–40.
Werner, C., Ryel, R.J., Correia, M.J. and Beyschlag, W. (2001b) Structural and functional variability within the canopy and its relevance for carbon gain and stress avoidance. Acta Oecologica – International Journal of Ecology **22**, 129–138.
Williams, L.E. (2010) Interaction of rootstock and applied water amounts at various fractions of estimated evapotranspiration (ET_c) on productivity of Cabernet Sauvignon. Australian Journal of Grape and Wine Research **16**, 334–434.
Williams, L.E. and Ayars, J.E. (2005) Grapevine water use and the crop coefficient are linear functions of the shaded area measured beneath the canopy. Agricultural and Forest Meteorology **132**, 201–211.
Williams, L.E. and Matthews, M.A. (1990) Grapevine. In: Irrigation of agricultural crops – agronomy monograph No. 30. Eds. B.A. Stewart and D.R. Nielson (ASA-CSSA-SSSA: Madison, WI, USA) pp. 1019–1059.
Williams, L.E., Dokoozlian, N.K. and Wample, R. (1994) Grape. In: Handbook of envrionmental physiology of fruit crops. Volume I Temperate crops. Eds. B. Schaffer and P.C. Anderson (CRC Press, Inc.: Boca Raton, FL, USA) pp. 85–133.
Williams, L.E., Grimes, D.W. and Phene, C.J. (2010a) The effects of applied water at various fractions of measured evapotranspiration on water relations and vegetative growth of Thompson Seedless grapevines. Irrigation Science **28**, 221–232.
Williams, L.E., Grimes, D.W. and Phene, C.J. (2010b) The effects of applied water at various fractions of measured evapotranspiration on reproductive growth and water productivity of Thompson Seedless grapevines. Irrigation Science **28**, 233–243.
Winkel, T. and Rambal, S. (1993) Influence of water stress on grapevines growing in the field: from leaf to whole plant response. Australian Journal of Plant Physiology **20**, 146–157.
Zufferey, V., Murisier, F. and Schultz, H.R. (2000) A model analysis of the photosynthetic response of *Vitis vinifera* L. cvs. Riesling and Chasselas leaves in the field. I. Interaction of age, light and temperature. Vitis **39**, 19–26.

Manuscript received: 7 February 2013
Accepted: 3 May 2013

Supporting information

Additional Supporting Information may be found in the online version of this article at the publisher's web-site: http://onlinelibrary.wiley.com/doi/10.1111/ajgw.12036/abstract

Figure S1. Measured parameters and modelled frequency distribution for leaf length. The figure represents the frequency of 1000 randomly generated parameters based on the mean and standard deviation derived from measurements taken at each grapevine shoot node.

Figure S2. Modelling the light environment within the canopy using a virtual movable photon flux density (PFD) sensor grid. The PFD sensor grid consists of 330 (11 × 30) 1-cm^2 diamond-shaped opaque (absorbance = 1) leaves organised as an array that can be placed at different heights in the canopy. The figures show different views of the array at different locations in the canopy. The PFD sensor grid allows a 3D mapping of the light environment within a simulated grapevine canopy.